



Article

A Ni₁₁ Coordination Cluster from the Use of the Di-2-Pyridyl Ketone/Acetate Ligand Combination: Synthetic, Structural and Magnetic Studies

Constantinos G. Efthymiou ^{1,2}, Ioannis Mylonas-Margaritis ³, Catherine P. Raptopoulou ⁴, Vassilis Psycharis ⁴, Albert Escuer ^{5,*}, Constantina Papatriantafyllopoulou ^{2,*} and Spyros P. Perlepes ^{3,6,*}

¹ Department of Chemistry, University of Cyprus, 1678 Nicosia, Cyprus; efthymiou.konstantinos@ucy.ac.cy or constantinos.efthymiou@nuigalway.ie

² Chemistry Department, Arts/Science Building, National University of Ireland Galway, University Road, Galway, Ireland

³ Department of Chemistry, University of Patras, 265 04 Patras, Greece; ioannismylonasmargaritis@gmail.com

⁴ Institute of Nanoscience and Nanotechnology, NCSR “Demokritos”, 153 10 Aghia Paraskevi Attikis, Greece; c.raptopoulou@inn.demokritos.gr (C.P.R.); v.psycharis@inn.demokritos.gr (V.P.)

⁵ Departament de Química Inorgànica and Institute of Nanoscience and Nanotechnology (IN2UB), Universitat de Barcelona, Diagonal 645, 08028 Barcelona, Spain

⁶ Institute of Chemical Engineering Sciences, Foundation for Research and Technology-Hellas (FORTH/ICE-HT), Platani, P.O. Box 1414, 265 04 Patras, Greece

* Correspondence: albert.escuer@ub.edu (A.E.); constantina.papatriantafyllopo@nuigalway.ie (C.P.); perlepes@patreas.upatras.gr (S.P.P.); Tel.: +34-93-4039141 (A.E.); +353-91-493462 (C.P.); +30-2610-996730 (S.P.P.)

Academic Editor: Núria Aliaga-Alcalde

Received: 21 May 2016; Accepted: 21 July 2016; Published: 2 August 2016

Abstract: The combined use of di-2-pyridyl ketone, (py)₂CO, and acetates (MeCO₂⁻) in nickel(II) chemistry in H₂O-MeCN under basic conditions (Et₃N) afforded the coordination cluster [Ni₁₁(OH)₆(O₂CMe)₁₂{(py)₂C(OH)(O)}₄(H₂O)₂] (**1**) in 80% yield, where (py)₂C(OH)(O)⁻ is the monoanion of the *gem*-diol form of (py)₂CO. The complex contains a novel core topology. The core of **1** comprises a central non-linear {Ni₃(μ₂-OH)₄}²⁺ subunit which is connected to two cubane {Ni₄(OH)(μ₃-OR)₂(μ₃-OR')⁴⁺ subunits [RO⁻ = (py)₂C(OH)(O)⁻ and R'O⁻ = MeCO₂⁻] via the OH⁻ groups of the former which become μ₃. The linkage of the Ni₃ subunit to each Ni₄ subunit is completed by two η¹:η¹:μ₂ and one η¹:η³:μ₄ MeCO₂⁻ groups. Peripheral ligation is provided by two terminal monodentate MeCO₂⁻ and two terminal aqua ligands. The (py)₂C(OH)(O)⁻ ligands adopt the η¹:η¹:η³:μ₃ coordination mode. From the twelve MeCO₂⁻ ligands, two are η¹, two η¹:η³:μ₄ and eight adopt the *syn*, *syn* η¹:η¹:μ₂ coordination mode; four of the latter bridge Ni^{II} centers at opposite faces of the cubane subunits. Complex **1** is the largest nickel(II)/(py)₂CO-based ligand coordination cluster discovered to date and has an extremely rare nuclearity (Ni₁₁) in the cluster chemistry of nickel(II). Variable-temperature, solid state dc susceptibility, and variable-field magnetization studies at low temperatures were carried out on complex **1**. The study of the data reveals an S = 3 ground state, which has been well rationalized in terms of known magnetostructural correlations and the structural features of **1**. An attempt has also been made to interpret the magnetic properties of the undecanuclear cluster in a quantitative manner using four exchange interaction parameters and the obtained J values are discussed. The role of H₂O in the solvent medium that led to **1**, and the high nickel(II) and acetate to di-2-pyridyl ketone reaction ratio employed for its preparation, on the nuclearity and identity of the cluster are critically analyzed.

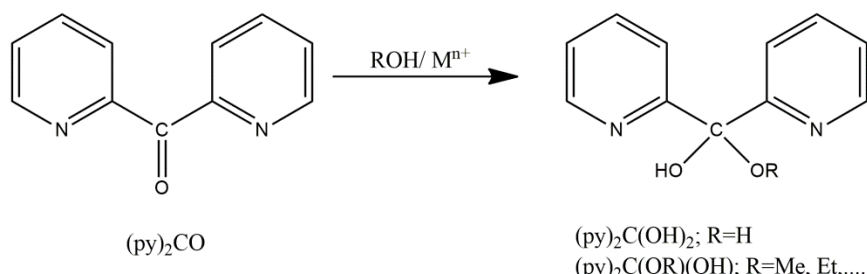
Keywords: ancillary carboxylate ligands; coordination clusters; di-2-pyridyl ketone-based ligands; nickel(II); magnetic properties; undecanuclearity in nickel(II) chemistry

1. Introduction

The chemistry of polynuclear complexes (coordination clusters) of 3d metals at intermediate oxidation states continues to attract intense attention from many research groups around the world. There are several reasons for this, but the three most important ones are the aesthetically pleasing structures that many such complexes possess [1,2], the search for models of metal-containing sites in biology [3,4], and various aspects of Molecular Magnetism—including high-spin molecules [5], Single-Molecule Magnets (SMMs) [6,7], and Molecular Magnetic Refrigerants [8,9].

Nickel(II) coordination clusters have been receiving increasing attention in the field of Molecular Magnetism. This 3d⁸ metal ion has shown promise in the synthesis of SMMs [7] and spin-phonon traps [10], with the former taking advantage of its significant single-ion anisotropy and the latter of its paramagnetic nature when the metal ion is confined in a highly symmetric cluster. These characteristics justify the interest of our groups in the chemistry of nickel(II) coordination clusters [11–15].

A synthetic challenge involves discovering simple and efficient approaches to the incorporation of many metal ions in a small, single molecular entity, simultaneously building useful magnetic properties into the resulting system. In the development of new synthetic routes to coordination clusters, the choice of primary organic ligands is always a key issue. A popular efficient ligand for the preparation of coordination clusters is di-2-pyridyl ketone, (py)₂CO (Scheme 1). Water and alcohols (ROH; R ≠ H) have been shown to add to the reactive carbonyl group upon coordination of the carbonyl oxygen and/or the 2-pyridyl nitrogen atoms, forming the ligands (py)₂C(OH)₂ [the *gem*-diol form of (py)₂CO] and (py)₂C(OR)(OH) [the hemiketal form of (py)₂CO], respectively (Scheme 1). The exciting structural chemistry of the (py)₂CO-based clusters [16,17] stems from the ability of the deprotonated ligands (py)₂C(O)₂²⁻, (py)₂C(OH)(O)⁻ and (py)₂C(OR)(O)⁻ to exhibit more than 15 distinct bridging coordination modes (with the simultaneous formation of one or two five-membered chelating rings) ranging from μ_2 to μ_5 .



Scheme 1. Di-2-pyridyl ketone, (py)₂CO, and its neutral *gem*-diol, (py)₂C(OH)₂, and hemiketal, (py)₂C(OR)(OH), forms. Note that (py)₂C(OH)₂, (py)₂C(OR)(OH) and their anionic derivatives (not shown) do not exist as free species, but exist only as ligands in their respective metal complexes. Mⁿ⁺ is a metal ion ($n = 2, 3$).

A modern trend for the synthesis of coordination clusters is the simultaneous employment of two bridging ligands in the reaction systems (a combination of ligands or ligand “blends”). The loss of a degree of synthetic control is more than compensated for by the vast diversity of structural types expected (and indeed observed) using a combination of ligands [18]. Often, the second ligand is a simple carboxylate ion, RCO₂⁻, which is famous for exhibiting a huge variety of coordination modes.

Restricting further discussion to Ni^{II}/(py)₂CO/MeCO₂⁻ chemistry, a variety of nickel(II) coordination clusters have been prepared from this general reaction system that contain both acetate groups and derivatives of (py)₂CO. These clusters are [Ni₄(O₂CMe)₄{(py)₂C(OH)(O)}₄] [19,20], [Ni₄(O₂CMe)₃{(py)₂C(OH)(O)}₄]X (X = ClO₄, MeCO₂) [20,21], [Ni₄(O₂CMe)₂{(py)₂C(OH)(O)}₄(H₂O)₂](ClO₄)₂ [20,22] and [Ni₉X₂(O₂CMe)₈{(py)₂C(O)₂}₄] (X = OH, N₃) [23]. The mononuclear complexes [Ni{(py)₂C(OH)₂}₂](O₂CMe)₂ [24] and [Ni(O₂CMe){(py)₂CO}{(py)₂C(OH)₂}](ClO₄) [20] have also been structurally characterized. All the above

mentioned Ni₄ and Ni₉ complexes were prepared in commercially available organic solvents that contain little H₂O (1%–3%). We wondered whether nickel(II) acetate clusters containing derivatives of (py)₂CO could be isolated from solvent mixtures comprising large amounts of H₂O. We also made another observation studying the literature: the MeCO₂⁻:(py)₂C(OH)(O)⁻, (py)₂C(O)₂²⁻ ratio in the clusters ranges from 1:2 to 2:1. We wondered if clusters containing higher such ratios could be prepared; we considered it possible that complexes with higher than 2:1 MeCO₂⁻:(py)₂C(OH)(O)⁻, (py)₂C(O)₂²⁻ ratios would also have high nuclearities. This paper gives positive answers to these two questions by describing the preparation, structural characterization, and magnetic study of a novel Ni₁₁ cluster prepared in a H₂O-rich organic solvent and having a 3:1 MeCO₂⁻:(py)₂C(OH)(O)⁻ stoichiometry.

2. Experimental Section

2.1. Materials and Physical Measurements

All manipulations were performed under aerobic conditions using materials and solvents (Alfa Aesar, Aldrich, Karlsruhe, Germany and Tanfrichen, Germany, respectively) as received. Elemental analyses (C, H, N) were performed by the University of Patras microanalytical service. FT-IR spectra (4000–400 cm⁻¹) were recorded using a Perkin-Elmer (Waltham, Ma, USA) 16PC FT-IR spectrometer with samples prepared as KBr pellets. Variable-temperature magnetic susceptibility measurements were performed using a DSM5 Quantum Design (San Diego, CA, USA) SQUID magnetometer operating at dc field of 0.3 T in the 300–30 K range and 0.02 T in the 30–2.0 K range to avoid saturation effects. Diamagnetic corrections were applied to the observed paramagnetic susceptibilities using Pascal's constants.

2.2. Synthesis of [Ni₁₁(OH)₆(O₂CMe)₁₂](py)₂C(OH)(O)₄(H₂O)₂]·1.2MeCN·3.2H₂O (**1**·1.2MeCN·3.2H₂O)

A solution of (py)₂CO (0.092 g, 0.50 mmol) in MeCN (5 mL) was slowly added to a solution of Ni(O₂CMe)₂·4H₂O (0.0248 g, 1.00 mmol) in H₂O (10 mL), and to the resulting green solution Et₃N (0.139 mL, 1.00 mmol) was added. The reaction mixture was stirred for a further 1 h, filtered to remove a small quantity of green solid and the filtrate was left undisturbed in a closed flask at room temperature. X-ray quality, green needles of the product were formed in a period of 4 d. The crystals were collected by filtration, washed with cold MeCN (2 × 1 mL) and Et₂O, and dried in air. Typical yields were in the range 75%–80% (based on the Ni^{II} available). The complex was satisfactorily analyzed as lattice MeCN-free, i.e., as **1**·3.2H₂O Anal. calc. for C₆₈H_{88.4}N₈Ni₁₁O_{43.2} (found values in parentheses): C 34.68 (34.81), H 3.79 (3.68), N 4.76 (4.71)%.

2.3. Single-Crystal X-ray Crystallography

A suitable crystal of **1**·1.2MeCN·3.2H₂O (0.05 × 0.08 × 0.30 mm) was mounted in air and covered with epoxy glue. Diffraction data were collected on a Rigaku (Tokyo, Japan) R-AXIS SPIDER Image Plate diffractometer at room temperature using graphite-monochromated Cu K α radiation. Data collection (ω -scans) and processing (cell refinement, data reduction, and Empirical absorption correction) were performed using the CrystalClear program package [25]. Important crystallographic data are listed in Table 1. The structures were solved by direct methods using SHELXS-97 [26] and refined by full-matrix least-squares techniques on F^2 with SHELXL-2014/6 [27]. Further experimental crystallographic details for **1**·1.2MeCN·3.2H₂O: $2\theta_{\max} = 130.0^\circ$, 693 parameters refined, $(\Delta/\sigma)_{\max} = 0.020$, $(\Delta\rho)_{\max}/(\Delta\rho)_{\min} = 0.78/-0.57$ e Å⁻³. All H atoms of the cluster molecule, except those of the acetate methyl groups, were located by difference maps and were refined isotropically. The H atoms of the methyl groups, were refined at calculated positions with $U_{\text{iso}}(\text{H}) = 1.5U_{\text{eq}}$ (carrier atom). All non-H atoms were refined anisotropically. The non-H atoms of the MeCN and H₂O solvent molecules were refined isotropically with partial occupancies. The H atoms of the solvent molecules were not located and were not included in the refinement. The X-ray crystallographic data for the complex in

a CIF format have been deposited with CCDC (reference number CCDC 1481082). They can be obtained free of charge at <http://www.ccdc.cam.ac.uk/conts/retrieving.html>, or from the Cambridge Crystallographic Data Centre, 12 Union Road, Cambridge CB2 1EZ, UK; Fax: +44-1223-336-033; or e-mail: deposit@ccdc.cam.ac.uk.

Table 1. Crystallographic data for cluster **1·1.2·MeCN·3.2H₂O**.

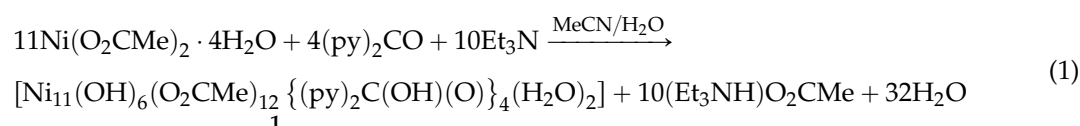
Formula	C _{70.4} H ₉₂ N _{9.2} Ni ₁₁ O _{43.2}
Formula weight	2404.14
Crystal system	monoclinic
Space group	I2/a
Radiation	Cu K α
T/K	293
a/ \AA	24.8808(5)
b/ \AA	15.2009(3)
c/ \AA	27.2265(6)
$\beta/^\circ$	96.521(6)
V/ \AA^3	10230.7(4)
Z	4
D _{calc} /g·cm ⁻³	1.561
μ/mm^{-1}	2.87
Reflns measured	60292
Reflns unique (R_{int})	8852
Reflns with $I > 2\sigma(I)$	7067
GOF on F^2	1.05
R_1 ^a [$I > 2\sigma(I)$]	0.0520
wR ₂ ^b (all data)	0.1611

$$^a R = \frac{\sum(|F_o| - |F_c|)}{\sum(|F_o|)}, ^b wR_2 = \left\{ \frac{\sum[w(F_0^2 - F_c^2)^2]}{\sum[w(F_0^2)^2]} \right\}^{1/2}.$$

3. Results and Discussion

3.1. Synthetic Comments and IR Discussion in Brief

A variety of Ni(O₂CMe)₂·4H₂O/(py)₂CO reaction systems in solvent mixtures comprising an organic solvent and H₂O were tested. Several parameters were systematically explored, such as the reaction ratio, the absence/presence of an external base, the nature of the organic solvent, the absence/presence of a counterion (Buⁿ₄N⁺, ClO₄⁻, PF₆⁻, ...), the temperature, the pressure (solvothermal conditions) and the crystallization method, before arriving at the optimized procedure described in the Experimental Section. The 2:1:2 Ni(O₂CMe)₂·4H₂O/(py)₂CO/Et₃N reaction mixture in MeCN-H₂O (1:2 v/v) gave a green solution from which were subsequently isolated green crystals of [Ni₁₁(OH)₆(O₂CMe)₁₂{(py)₂C(OH)(O)}₄(H₂O)₂]·1.2MeCN·3.2H₂O (**1·1.2MeCN·3.2H₂O**) in a high yield (~80%). Assuming that **1** is the only product from this reaction system, its formation can be summarized by Equation (1):



Increasing the Ni^{II}:(py)₂CO reaction ratio in MeCN-H₂O from 2:1 to 3:1 gives again the cluster **1** at comparable yields. It should be mentioned at this point that the absence of Et₃N from the reaction mixture (in the same solvent system) does not lead to **1**, but—instead—to a green non-crystalline powder which could not be characterized. We could not isolate nickel(II) acetate clusters containing the doubly deprotonated derivative of the *gem*-diol form of (py)₂CO, i.e., Ni^{II}/MeCO₂⁻/(py)₂C(O)₂²⁻

complexes, in H_2O -containing organic solvents, even performing hundreds of reactions at various concentrations of external bases and adding bulky cations in the reaction mixtures.

In the IR spectrum of **1**, the medium-to-strong intensity broad band covering the whole $3550\text{--}3150\text{ cm}^{-1}$ region and exhibiting several sub-maxima is assigned to the $\nu(\text{OH})$ vibrations of the coordinated hydroxide (OH^-), $(\text{py})_2\text{C}(\text{OH})(\text{O})^-$ and aqua groups, as well as to this vibration from the lattice H_2O molecules. The spectrum does not exhibit a band in the region of the carbonyl stretching vibration [$\nu(\text{CO})$] as expected from the absence of carbonyl-containing $(\text{py})_2\text{CO}$ ligands in the complex, with the nearest band at $\sim 1595\text{ cm}^{-1}$ assigned to a pyridyl stretching vibration—this band also has a $\nu_{\text{as}}(\text{CO}_2)$ character—raised from 1582 cm^{-1} upon coordination; this spectroscopic feature has been observed earlier [28] upon complex formation involving hydration of $(\text{py})_2\text{CO}$. Several bands appear in the $1600\text{--}1380$ region; these are due to contributions from the stretching vibrations of the pyridyl ring, the $\nu_{\text{as}}(\text{CO}_2)$ and $\nu_{\text{s}}(\text{CO}_2)$ modes of the MeCO_2^- ligands (which are of three different types, *vide infra*), and the $\delta(\text{CH}_3)$ vibrations. An overlap is possible, and this renders exact assignments and studies of the coordination shifts rather impossible.

3.2. Description of Structure

The molecular structure of **1**· $1.2\text{MeCN}\cdot 3.2\text{H}_2\text{O}$ is shown in Figure 1. The coordination modes of all the ligands present in the cluster are shown in Figure 2; other structural plots of the compound are presented in Figures 3–6.

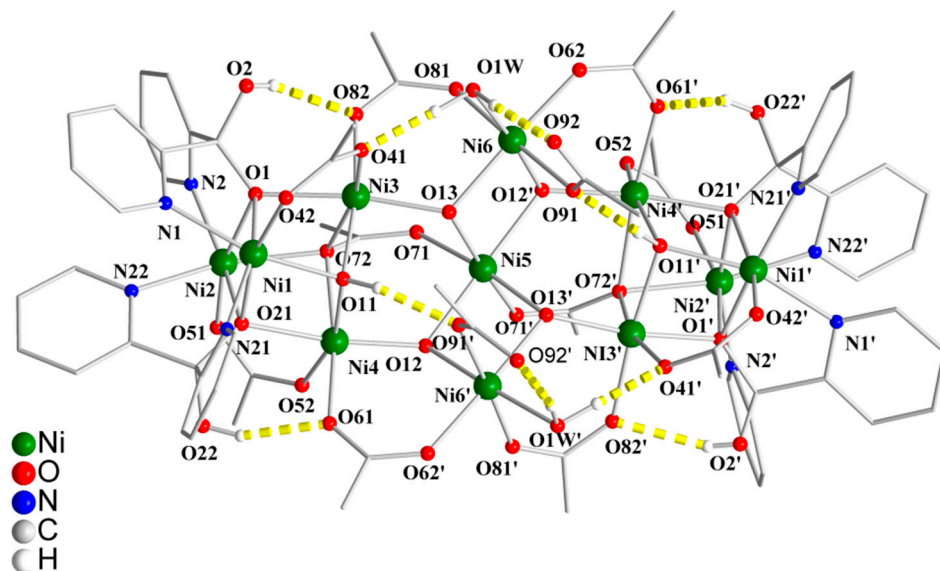


Figure 1. Partially labelled plot of the molecule $[\text{Ni}_{11}(\text{OH})_6(\text{O}_2\text{CMe})_{12}\{(\text{py})_2\text{C}(\text{OH})(\text{O})\}_4(\text{H}_2\text{O})_2]$ that is present in the structure of **1**· $1.2\text{MeCN}\cdot 3.2\text{H}_2\text{O}$. The thick dashed yellow lines indicate the intramolecular H bonds. Symmetry operation used to generate equivalent atoms: $(') -x + \frac{1}{2}, y, -z + 2$.

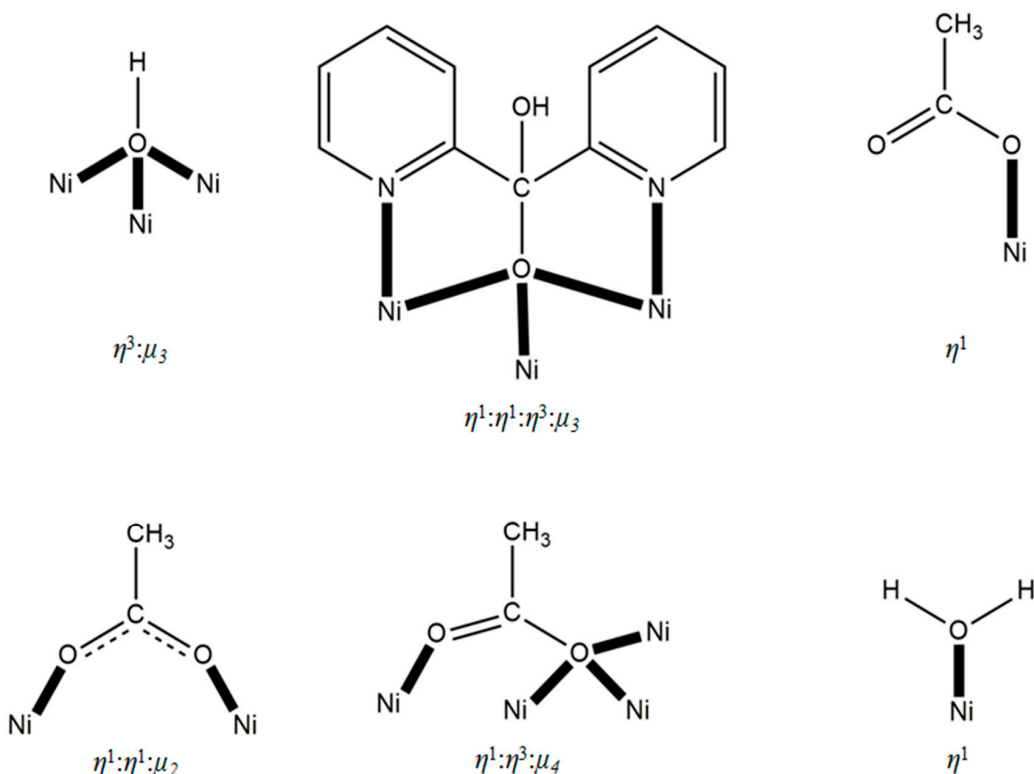


Figure 2. The coordination modes of all the ligands that are present in the structure of **1·1.2MeCN·3.2H₂O** and the η/μ notation that describes these modes.

Selected interatomic distances and bond angles, and details of the H-bonding interactions in the complex are shown in Tables 2 and 3, respectively.

Table 2. Selected interatomic distances (\AA) and bond angles ($^\circ$) for cluster $[\text{Ni}_{11}(\text{OH})_6(\text{O}_2\text{CMe})_{12}\{(\text{py})_2\text{C}(\text{OH})(\text{O})\}_4(\text{H}_2\text{O})_2]\cdot1.2\text{MeCN}\cdot3.2\text{H}_2\text{O}$ (**1·1.2MeCN·3.2H₂O**).

Interatomic Distances (\AA) ^a			
Ni1…Ni2	3.024(1)	Ni1…O1	2.045(3)
Ni1…Ni3	2.928(1)	Ni1…O21	2.106(3)
Ni1…Ni4	3.285(1)	Ni1…N1	2.151(4)
Ni2…Ni3	3.440(1)	Ni2…O21	1.997(3)
Ni2…Ni4	3.002(1)	Ni2…O72	2.229(3)
Ni3…Ni4	3.154(1)	Ni2…N22	2.143(3)
Ni5…Ni6	3.083(1)	Ni3…O11	2.014(3)
Ni1…Ni5	5.763(1)	Ni3…O72	2.214(3)
Ni2…Ni5	5.496(1)	Ni3…O82	2.017(3)
Ni3…Ni5	3.457(1)	Ni4…O11	2.018(3)
Ni4…Ni5	3.634(1)	Ni4…O52	2.066(3)
Ni1…Ni6'	5.831(1)	Ni4…O72	2.258(3)
Ni2…Ni6'	6.396(1)	Ni5…O12	2.099(3)
Ni3…Ni6'	4.897(1)	Ni5…O13	2.050(3)
Ni4…Ni6'	3.477(1)	Ni5…O71	2.074(3)
Ni1…Ni1'	10.859(1)	Ni6…O12'	2.053(3)
Ni1…Ni2'	8.599(1)	Ni6…O81	2.078(3)
Ni2…Ni4'	8.855(1)	Ni6…O1W	2.090(3)
Bond Angles ($^\circ$) ^a			
O1–Ni1–N21	158.2(1)	Ni1–O1–Ni3	89.1(1)
O11–Ni1–N1	160.7(1)	Ni2–O1–Ni3	109.3(1)

Table 2. Cont.

Bond Angles ($^{\circ}$) ^a			
O21–Ni1–O42	165.5(1)	Ni1–O11–Ni3	92.1(1)
O1–Ni2–O51	164.4(1)	Ni1–O11–Ni4	107.6(1)
O21–Ni2–N2	158.8(1)	Ni3–O11–Ni4	102.9(1)
O72–Ni2–N22	166.1(1)	Ni1–O21–Ni2	95.0(1)
O1–Ni3–O13	171.0(1)	Ni1–O21–Ni4	102.8(1)
O11–Ni3–O82	171.8(1)	Ni2–O21–Ni4	94.3(1)
O41–Ni3–O72	166.1(1)	Ni2–O72–Ni3	101.5(1)
O11–Ni4–O52	161.2(1)	Ni2–O72–Ni4	84.0(1)
O12–Ni4–O21	172.1(1)	Ni3–O72–Ni4	89.7(1)
O61–Ni4–O72	172.6(1)	Ni4–O12–Ni5	125.3(2)
O12–Ni5–O12'	175.6(2)	Ni4–O12–Ni6'	118.5(1)
O13–Ni5–O71'	172.6(1)	Ni5–O12–Ni6'	95.9(1)
O12'–Ni6–O1W	174.4(1)	Ni3–O13–Ni5	117.1(2)
O13–Ni6–O62	175.8(1)	Ni3–O13–Ni6	121.4(2)
O81–Ni6–O91	178.0(1)	Ni5–O13–Ni6	97.8(1)
Ni1–O1–Ni2	94.0(1)	-	-

^a Symmetry operation used to generate equivalent atoms: ('') $-x + \frac{1}{2}, y, -z + 2$.

Complex **1·1.2MeCN·3.2H₂O** crystallizes in the monoclinic space group *I*2/*a*. Its structure consists of undecanuclear cluster [Ni₁₁(OH)₆(O₂CMe)₁₂{(py)₂C(OH)(O)}₄(H₂O)₂], and solvate MeCN and H₂O molecules; the latter two will not be further discussed. The cluster molecule possesses a crystallographic two-fold symmetry axis passing through Ni5; thus, there are six crystallographically independent Ni^{II} atoms. The cluster molecule consists of 11 Ni^{II} atoms held together by six μ_3 -OH[−] ions (O11, O12, O13, O11', O12', O13'), four η^1 : η^1 : η^3 : μ_3 (py)₂C(OH)(O)[−] ligands (the triply-bridging oxygen atoms are O1, O21 and their symmetry equivalent), and two η^1 : η^3 : μ_4 (their oxygen atoms are O71/O72 and O71'/O72') and eight *syn, syn* η^1 : η^1 : μ_2 (their oxygen atoms are O41/O42, O51/O52, O61/O62', O81/O82 and symmetry equivalent) MeCO₂[−] groups; where multiple *n* values are given, they are indicating the hapticity of each donor atom rather than the whole (py)₂C(OH)(O)[−] or MeCO₂[−] group, that is, the number of Ni^{II} atoms to which a donor atom is attached. Peripheral ligation is provided by two terminal monodentate MeCO₂[−] groups (their ligating atoms are O91, O91') and two terminal aqua ligands (O1W, O1W') on Ni6 and Ni6'. The core (Figure 3) can be described as a central, non-linear {Ni₃(μ₂-OH)₄}²⁺ subunit linked to two {Ni₄(μ₃-OH)(μ₃-OR)₂(μ₃-OR')⁴⁺ distorted cubane subunits [RO[−] = (py)₂C(OH)(O)[−] and R'O[−] = MeCO₂[−]] via two OH[−] groups of the former to each of the latter; thus, the four OH[−] groups of the trinuclear subunit become μ_3 . The linkage of the central, non-linear Ni₃ submit to each Ni₄ subunit is completed by two η^1 : η^1 : μ_2 and one η^1 : η^3 : μ_4 MeCO₂[−] ligands. The whole core is {Ni₁₁(μ₃-OH)₆(μ₃-OR)₄(μ₃-OR')₂}¹⁰⁺.

Table 3. Intra- and intermolecular H bonds in the crystal structure of cluster **1·1.2MeCN·3.2H₂O** ^{a,b,c}.

D–H…A	D–H (Å)	H…A (Å)	D…A (Å)	D–H…A (°)
Intramolecular				
O11–H(O11)…O91'	0.90(5)	1.93(5)	2.793(4)	159(4)
O2–H(O2)…O82	0.71(5)	2.08(5)	2.759(5)	161(6)
O22–H(O22)…O61	0.84(6)	1.98(6)	2.763(4)	157(6)
O1W–HA(O1W)…O41	0.97(6)	1.76(6)	2.718(4)	169(5)
O1W–HB(O1W)…O92	0.86(5)	1.80(5)	2.637(6)	165(5)
Intermolecular				
C8–H8…O1W''	0.91(5)	2.49(5)	3.212(7)	136(4)
C30–H30…O42'''	1.10(6)	2.45(6)	3.495(6)	158(4)

^a D = donor, A = acceptor; ^b Atoms C8 and C30 are aromatic carbon atoms of the (py)₂C(OH)(O)[−] ligands;

^c Symmetry codes: ('') $-x + 1/2, y, -z + 2$; ('') $-x + 1/2, -y + 1/2, -z + 3/2$; ('''') $-x, y - 1/2, -z + 3/2$.

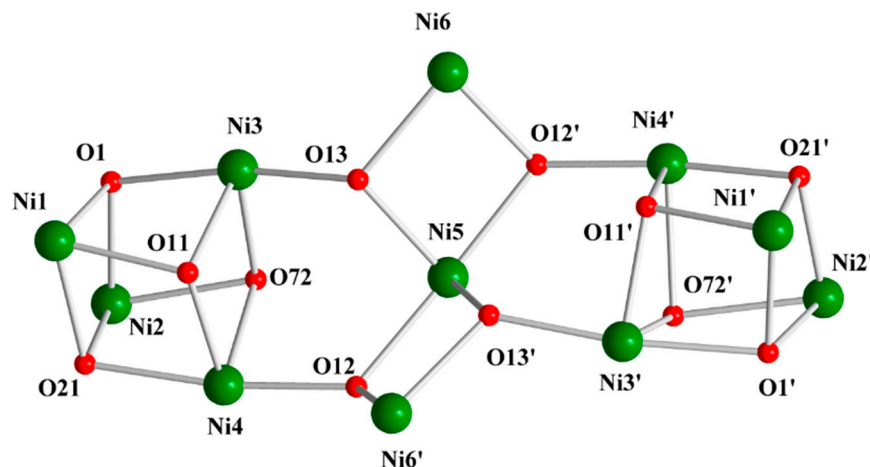


Figure 3. The $\{Ni_{11}(\mu_3\text{-OH})_6(\mu_3\text{-OR})_4(\mu_3\text{-OR}')_2\}^{10+}$ core of $1\cdot1\cdot2\text{MeCN}\cdot3\cdot2\text{H}_2\text{O}$, where $RO^- = (\text{py})_2\text{C}(\text{OH})(\text{O})^-$ and $R'\text{O}^- = \text{MeCO}_2^-$. Atoms O11, O12, O13, O11', O12', O13' are hydroxido oxygen atoms, while O72, O72' are the triply-bridging oxygen atoms of the two symmetry-related $\eta^1\text{:}\eta^3\text{:}\mu_4$ MeCO_2^- groups; atoms O1, O21, O1', O21' are the triply-bridging oxygen atoms of the $\eta^1\text{:}\eta^1\text{:}\eta^3\text{:}\mu_3$ $(\text{py})_2\text{C}(\text{OH})(\text{O})^-$ ligands.

In the crystallographically independent, distorted cubane subunit, the four Ni^{II} atoms ($\text{Ni}1$, $\text{Ni}2$, $\text{Ni}3$, $\text{Ni}4$) and the deprotonated $\mu_3\text{-O}$ atoms [$\text{O}11$ from a hydroxido group, $\text{O}1$ and $\text{O}21$ from the $(\text{py})_2\text{C}(\text{OH})(\text{O})^-$ ligands, $\text{O}72$ from a MeCO_2^- ion] occupy alternate vertices of the cube. Thus, the subunit consists of two interpenetrating concentric tetrahedra, one of four metal ions and the other of four triply-bridging oxygen atoms. The two opposite $\text{Ni}1\text{O}1\text{Ni}3\text{O}11$ and $\text{Ni}2\text{O}2\text{Ni}4\text{O}72$ faces of the cube are capped by two *syn, anti* $\eta^1\text{:}\eta^1\text{:}\mu_2$ MeCO_2^- groups ($\text{O}41/\text{O}42$ and $\text{O}51/\text{O}52$, respectively), that lie across the face diagonals. As a result the $\text{Ni}1\cdots\text{Ni}3$ [2.928(1) Å] and $\text{Ni}2\cdots\text{Ni}4$ [3.002(1) Å] are shorter than the other intracubane $\text{Ni}\cdots\text{Ni}$ distances [3.024(1)–3.440(1) Å] and the $\text{Ni}-\text{O}-\text{Ni}$ angles [84.0(1)°–94.3(1)°] are more acute than the four faces not bridged in this fashion. This means that from the eight $\eta^1\text{:}\eta^1\text{:}\mu_2$ acetate groups, four bridge Ni^{II} ions within the cubane subunits and four ($\text{O}81/\text{O}82$, $\text{O}61/\text{O}62'$ and their symmetry equivalent) bridge $\text{Ni}6$, $\text{Ni}6'$ of the central Ni_3 subunit and metal ions ($\text{Ni}3$, $\text{Ni}4$ and their symmetry equivalent) that belong to the cubane subunits. There are two types of $\text{Ni}-\text{O}$ (hydroxido, alkoxido, acetato) bonds for each metal ion within the cubane subunits: the first is rather short at an average distance of 2.019(3) Å, the second bond is of intermediate strength at an average distance of 2.093(3) Å, whereas the third bond is longer at an average bond length of 2.202(3) Å. The cube deviates significantly from the ideal geometry. The internal cube angles ($\text{O}-\text{Ni}-\text{O}$) at the metal vertices average 81.3(1)°, whereas the corresponding angles at the triply-bridging oxygen corners ($\text{Ni}-\text{O}-\text{Ni}$) are much larger averaging 96.9(1)°. This deviation arises primarily from the different nature of the $\mu_3\text{-O}$ atoms and the resulting different $\text{Ni}-(\mu_3\text{-O})$ bond lengths for a given metal ion, as well as from the presence of two bridging acetates within the cube.

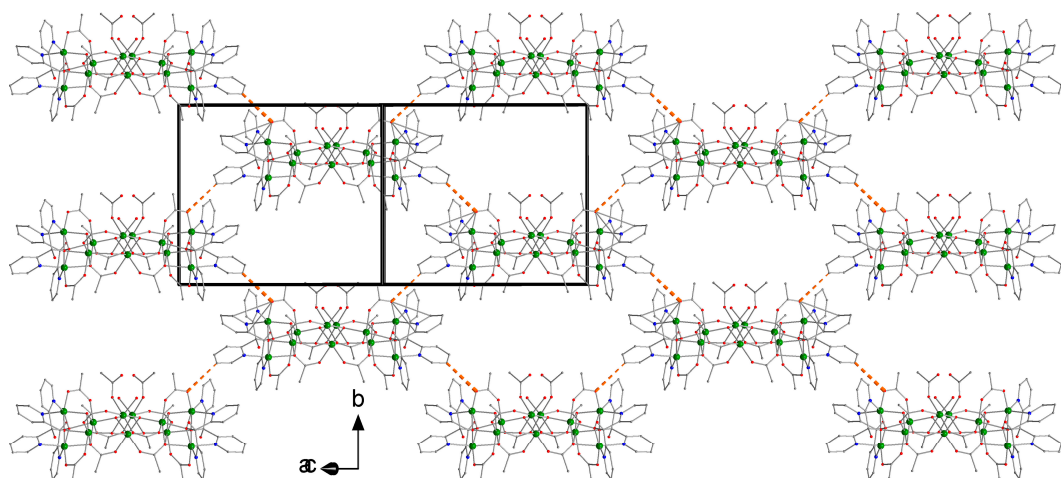


Figure 4. Layers formed by cluster molecules of **1** parallel to the (10–1) plane. The thick dashed orange lines indicate the intermolecular C30–H30…O42 H bond (and its symmetry equivalent); see Table 3 for metric parameters. Atom C30 belongs to a $(\text{py})_2\text{C}(\text{OH})(\text{O})^-$ ligand and O42 is a coordinated acetato oxygen.

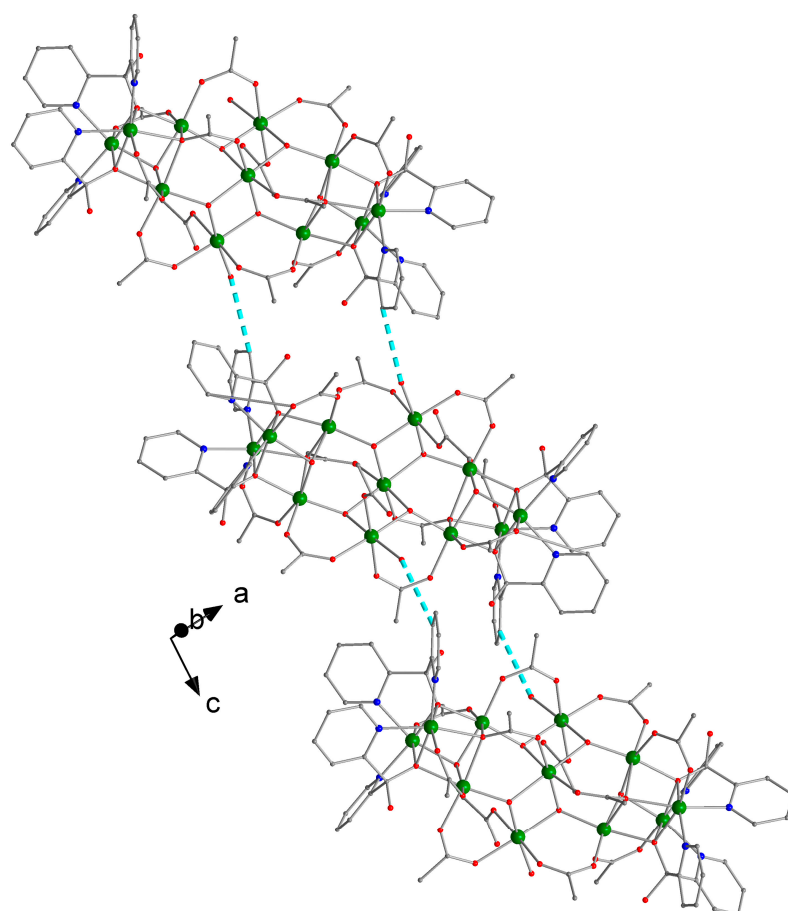


Figure 5. Chains formed by cluster molecules of **1** along the *c* axis. The thick dashed turquoise lines indicate the intermolecular C8–H8…O1W H bond (and its symmetry equivalent); see Table 3 for metric parameters. Atom C8 belongs to a $(\text{py})_2\text{C}(\text{OH})(\text{O})^-$ ligand and O1W is the oxygen atom of the coordinated H_2O molecule.

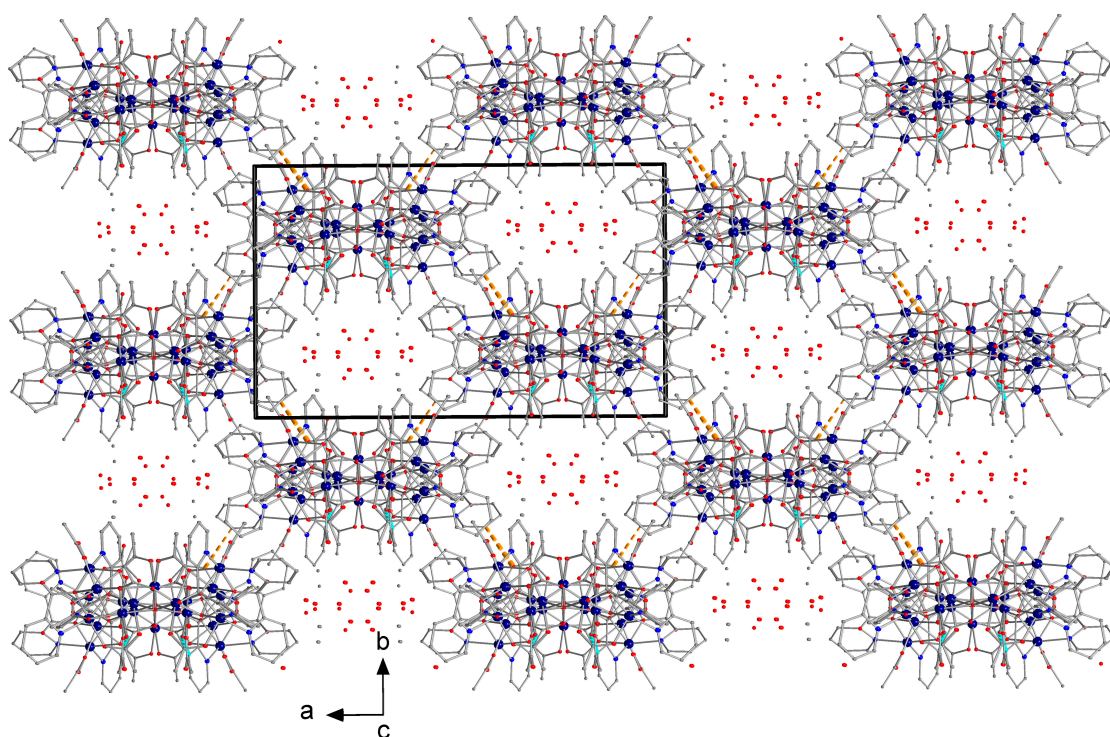


Figure 6. A partial plot of the 3D architecture of **1**·1.2MeCN·3.2H₂O along the *c* axis showing the channels formed; the dots in the channels indicate the positions of solvent molecules.

Atoms Ni3, Ni4, Ni5, and Ni6 are bound to an O₆ set of donor atoms, and Ni1 and Ni2 form NiO₄N₂ chromophores. Thus, all the Ni^{II} atoms are six-coordinate with distorted octahedral geometries, the main distortion arising from the relatively small bite angle of the chelating NNiO parts of the (py)₂C(OH)(O)⁻ groups [75.9(1)[°]–80.0(1)[°]]. The Ni–N and Ni–O bond lengths lie well within the ranges reported for other octahedral nickel(II) complexes with O- and/or N-ligation [11–15,18–24]. The Ni(2, 3 ,4) bond distances to the triply-bridging oxygen atom (O72) of the η¹:η¹:μ₄ MeCO₂⁻ group [average 2.234(3) Å] are significantly larger than the other Ni–O (acetate) bond lengths. Although Ni₄ complexes containing the cubane core are well known in the literature [13,14,20–22], the {Ni₄(μ₃-OH)(μ₃-OR)₂(μ₃-OR')⁴⁺} core with three different types of triply-bridging oxygen atoms present in **1** has not been observed either in a discrete Ni₄ cluster or as a recognizable subfragment of higher nuclearity nickel(II) clusters.

Within the cluster molecule, there are five H bonds of intermediate strength. The donors are the intracubane hydroxido group (O11), the unbound –OH groups of the (py)₂C(OH)(O)⁻ ligands and the coordinated H₂O molecule (and their symmetry equivalent). The acceptors are the non-coordinated (O92) and coordinated (O41, O61, O82, O91') acetato oxygen atoms (and their symmetry equivalent). The Ni₁₁ molecules are arranged in layers parallel to the (10-1) plane through C30–H30…O42 H bonds (Figure 4). Cluster molecules belonging to different layers interact through C8–H8…O1W H bonds forming chains along the *c* axis. Viewing down the *c* axis, we observe that cluster molecules in neighboring layers are arranged on this axis in an eclipsed way forming channels that are occupied by solvent molecules.

Complex **1** is the largest nickel(II)/di-2-pyridyl ketone-based coordination cluster discovered. While the number of high-nuclearity, non-organometallic complexes of nickel(II) with O- and/or N-based ligands and without metal-metal bonding continues to grow rapidly [11,15,29–33] (the record nuclearity is 26 [29]), some nuclearities remain rare. Undecanuclear nickel(II) complexes are particularly rare, and complex **1** thus becomes a new member of the small family of Ni₁₁ clusters [34–38]; the metal topology and core of **1** are novel.

3.3. Magnetochemistry

Direct current (dc) magnetic susceptibility data (χ_M) on a dried polycrystalline, analytically pure sample of **1** were collected in the 2.0–300 K range. The data are plotted as $\chi_M T$ vs. T product in Figure 7. The room temperature $\chi_M T$ value is $14.17 \text{ cm}^3 \cdot \text{K} \cdot \text{mol}^{-1}$, slightly higher than the spin-only value of $13.31 \text{ cm}^3 \cdot \text{K} \cdot \text{mol}^{-1}$ (with $g = 2.2$) expected for a cluster of 11 non-interacting $S = 1$ Ni^{II} centers. The $\chi_M T$ product decreases gradually with decreasing temperature in the range 300–100 K and rapidly in the range 100–10 K to reach a minimum value of $6.11 \text{ cm}^3 \cdot \text{K} \cdot \text{mol}^{-1}$, before increasing slightly at lower temperatures to reach a final value of $6.39 \text{ cm}^3 \cdot \text{K} \cdot \text{mol}^{-1}$ at 2.0 K. Magnetization experiments up to 5 T at 2.0 K (inset of Figure 7) show a saturation value of $M/N\mu_B = 6.4$. Fit of the reduced magnetization (Figure 8) in the 0–5 T and 1.8–6.8 K ranges gave a good agreement for an $S = 3$ spin level and $g = 2.10$. The D value of 0.6 cm^{-1} is indicative of a weak anisotropy of the ground state and consequently no out-of-phase susceptibility signals were seen in the ac experiments. Thus, the low temperature $\chi_M T$ value and the Brillouin shape of the magnetization plot allow us to propose an unambiguous well-isolated $S = 3$ ground state for compound **1**.

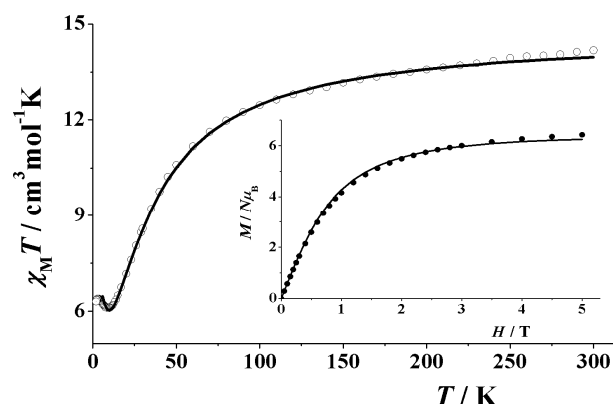


Figure 7. $\chi_M T$ vs. T and $M/N\mu_B$ vs. dc field at 2 K plots (inset) for compound **1**. Solid lines are the fits of the data; see the text for the fit parameters.

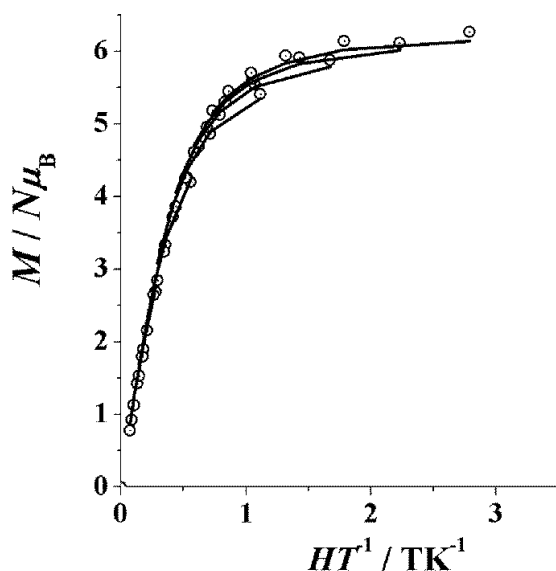
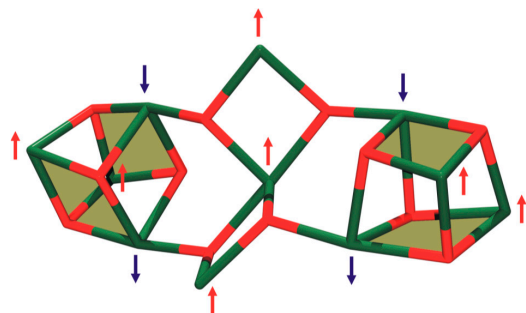


Figure 8. Reduced magnetization plots for compound **1**; the data were collected at increments of 1 K in the 1.8–6.8 K range under fields up to 5 T. Solid lines are the fits of the experimental data that give $S = 3$ and $D = 0.6 \text{ cm}^{-1}$.

In order to provide a qualitative explanation of the magnetic properties of **1**, we assume as main interactions those provided by the monatomic oxygen bridges, which can be analyzed based on well-established magnetostructural correlations in nickel(II) complexes [11–15,18,20–22,34,39–49]. The linkage between the external cubanes and the central Ni_3 subunit involves four $\text{Ni}-\text{O}(\text{hydroxido})-\text{Ni}$ units (Figure 3) with bond angles in the 117.1° – 125.3° ; these angles are expected to propagate antiferromagnetic exchange interactions. The most important parameter in the magnetostructural correlations of Ni_4 cubanes with four triply-bridging oxygen atoms has been reported [20,39–49] to be the average $\text{Ni}-\text{O}-\text{Ni}$ angle of a cubane face. A ferromagnetic exchange is observed for $\text{Ni}-\text{O}-\text{Ni}$ angles lower than 99° and the positive coupling value increases as the angle decreases. However, $\text{Ni}-\text{O}-\text{Ni}$ angles in the vicinity of, or larger than, 99° lead to antiferromagnetic interactions and the absolute value increases as the angle increases. It has also been established [49] that if a cubane possesses at least two opposite faces with average $\text{Ni}-\text{O}-\text{Ni}$ bond angles close to 105° , the antiferromagnetic $\text{Ni}\cdots\text{Ni}$ interactions for these faces prevail over the ferromagnetic $\text{Ni}\cdots\text{Ni}$ interactions in the other faces leading to $S = 0$ for the whole cubane. This is the case in cluster **1**. The $\text{Ni}_1\text{O}_1\text{Ni}_2\text{O}_2$, $\text{Ni}_3\text{O}_1\text{Ni}_4\text{O}_7$, $\text{Ni}_1\text{O}_1\text{Ni}_3\text{O}_1$, $\text{Ni}_2\text{O}_2\text{Ni}_4\text{O}_7$, $\text{Ni}_2\text{O}_1\text{Ni}_3\text{O}_7$, and $\text{Ni}_1\text{O}_1\text{Ni}_4\text{O}_2$ faces of the crystallographically-independent Ni_4 cubane subunit have average $\text{Ni}-\text{O}-\text{Ni}$ bond angles of 94.5° , 96.3° , 90.6° , 89.2° , 105.4° , and 105.2° , respectively, and a local $S = 0$ value is expected for this subunit (and its symmetry equivalent). Thus the observed $S = 3$ ground state for the whole cluster should arise from ferromagnetic exchange interactions within the central Ni_3 subunit. The small values of 97.8° and 95.9° for the $\text{Ni}_5-\text{O}_1\text{Ni}_6$ (and its symmetry equivalent $\text{Ni}_5-\text{O}_1\text{Ni}_6'$) and $\text{Ni}_5-\text{O}_2\text{Ni}_6$ (and its symmetry equivalent $\text{Ni}_5-\text{O}_2\text{Ni}_6'$) bond angles, respectively, fully justify the ferromagnetic $\text{Ni}_5\cdots\text{Ni}_6/\text{Ni}_5\cdots\text{Ni}_6'$ exchange interactions. A schematic plot of the core of **1** with the proposed alignment of the local spins is shown in Scheme 2. This alignment, based on the above discussion, leads to the $S = 3$ ground state.

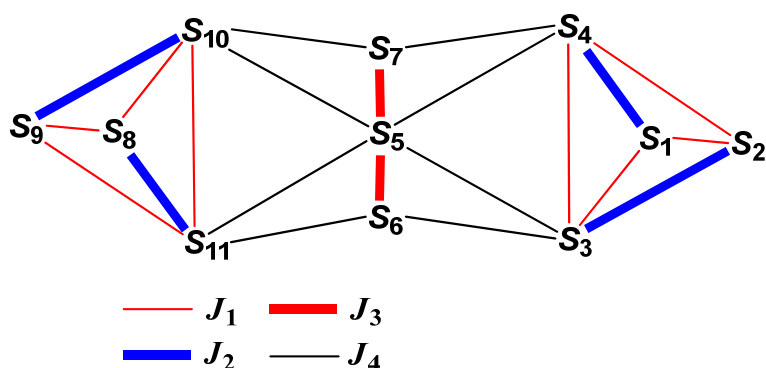


Scheme 2. Schematic plot of the core of **1** with the proposed alignment of the local spins that results in the $S = 3$ ground state. The faces of the two cubes depicted in green color correspond to the $\text{Ni}_2\text{O}_1\text{Ni}_3\text{O}_7$ and $\text{Ni}_1\text{O}_1\text{Ni}_4\text{O}_2$ (and their symmetry equivalent) cubane faces of the real structure that are characterized by large average $\text{Ni}-\text{O}-\text{Ni}$ angles (105.4° and 105.2° , respectively). These bond angles are responsible for the dominant antiferromagnetic coupling within each cubane subunit. The central trimeric $\{\text{Ni}(\text{OH})_2\text{Ni}(\text{OH})_2\text{Ni}\}^{2+}$ subunit is characterized by small $\text{Ni}-\text{O}-\text{Ni}$ angles (95.9° , 97.8°) which are compatible with weak ferromagnetic coupling. The coupling between the central Ni_3 subunit and the external cubanes should be the strongest interaction, antiferromagnetic in nature, due to the large $\text{Ni}-\text{O}-\text{Ni}$ bond angles involved (117.1° – 125.3°).

In order to check the above mentioned qualitative approach, a fit of the experimental magnetic susceptibility data was attempted on the basis of the exchange interactions shown in Scheme 3 and the derived Hamiltonian of Equation (2):

$$\begin{aligned} H = & -2J_1(S_1 \cdot S_2 + S_1 \cdot S_3 + S_2 \cdot S_4 + S_3 \cdot S_4 + S_8 \cdot S_9 + S_8 \cdot S_{10} + S_9 \cdot S_{11} + S_{10} \cdot S_{11}) \\ & -2J_2(S_1 \cdot S_4 + S_2 \cdot S_3 + S_8 \cdot S_{11} + S_9 \cdot S_{10}) - 2J_3(S_5 \cdot S_6 + S_5 \cdot S_7) - 2J_4(S_3 \cdot S_5 + \\ & S_3 \cdot S_6 + S_4 \cdot S_5 + S_4 \cdot S_7 + S_5 \cdot S_{10} + S_7 \cdot S_{10} + S_5 \cdot S_{11} + S_6 \cdot S_{11}) \end{aligned} \quad (2)$$

The coupling constant J_1 corresponds to the intracubane exchange interactions characterized by low Ni–O–Ni bond angles (the Ni1…Ni2, Ni3…Ni4, Ni1…Ni3, Ni2…Ni4 and their symmetry equivalent exchange interactions in the real structure), J_2 corresponds to the intracubane exchange interactions in two opposite faces of the cubane characterized by large Ni–O–Ni bond angles (the Ni1…Ni4, Ni2…Ni3 and their symmetry equivalent exchange interactions in the real structure), J_3 corresponds to the intratrimer exchange interactions (the Ni5…Ni6 and Ni5…Ni6' exchange interactions in the real structure) and J_4 corresponds to the exchange interactions between the central trinuclear fragment and the two cubanes (the Ni6…Ni3, Ni5…Ni3, Ni5…Ni4, Ni6'…Ni4 and their symmetry equivalent interactions in the real structure). The fit performed with the PHI program [50] gives the best-fit parameters $J_1 = +2.7 \text{ cm}^{-1}$, $J_2 = -4.8 \text{ cm}^{-1}$, $J_3 = +1.9 \text{ cm}^{-1}$, $J_4 = -6.4 \text{ cm}^{-1}$, $g = 2.31$ with $R = 1.9 \times 10^{-6}$. The absolute J values are not fully reliable due to the possibilities of other solutions that could give reasonable fits, but their signs and relative magnitudes are in excellent agreement with the expected exchange interactions based on the structural characteristics of **1**.



Scheme 3. Magnetic exchange coupling scheme for **1**. The J_1 , J_2 , J_3 , and J_4 interactions are fully described in the text. The spin carriers S_1 , S_2 , S_3 , S_4 , S_5 , S_6 , S_7 , S_8 , S_9 , S_{10} , and S_{11} correspond to the metal centers Ni1, Ni2, Ni3, Ni4, Ni5, Ni6, Ni6', Ni1', Ni2', Ni3', and Ni4', respectively, of the real structure.

4. Concluding Comments and Perspectives

The present work extends the body of results that emphasize the ability of the anionic forms of $(\text{py})_2\text{CO}$ to form interesting structural types in the chemistry of 3d-metal coordination clusters. The use of both $(\text{py})_2\text{CO}$ and MeCO_2^- in a reaction with nickel(II) in $\text{H}_2\text{O}-\text{MeCN}$ under basic conditions has led to cluster **1**, the highest nuclearity $\text{Ni}^{II}/(\text{py})_2\text{CO}$ -based ligand complex to date, showing that $(\text{py})_2\text{CO}$ can indeed support high nuclearity chemistry when combined with appropriate ancillary ligands, such as simple carboxylates. The cluster exhibits some novel features, the most impressive one being the simultaneous presence of three different types of acetate coordination. It is also impressive that oxygen atoms of three ligands, i.e., OH^- , MeCO_2^- , and $(\text{py})_2\text{C}(\text{OH})\text{O}^-$, are triply-bridging. The work described above also demonstrates the synthetic novelty that arises when MeCO_2^- is used in conjunction with $(\text{py})_2\text{CO}$ in solvent media containing large concentrations of H_2O and when the metal ion is in excess. Concerning the role of H_2O , it is obvious that H_2O is responsible for the formation of large concentrations of OH^- ions in basic media that favor products completely different compared with those seen previously. As far as the role of the excess of the metal ion in the reaction mixture is concerned, this favors high nuclearities and permits the ancillary ligand (the MeCO_2^- in the present case) to play a decisive role in the construction of the cluster, as observed in **1** in which the ratio of ancillary ligand:primary ligand in the product is 3. The magnetic study revealed that **1** possesses an $S = 3$ around state which has been rationalized in terms of the structural characteristics of the cluster, and known magnetostructural correlations for dinuclear and polynuclear nickel(II) complexes. An attempt has also been made to interpret the magnetic properties of **1** in a quantitative manner using four exchange interactions, and the obtained signs and relative magnitudes for the coupling constants

are in perfect agreement with what would be expected. The four Ni^{II} atoms in each cubane subunit are antiferromagnetically coupled and the $S = 3$ value in the ground state of the cluster thus derives from the ferromagnetic alignment of the local spins in the central Ni₃ subunit.

We have no reason to believe that this research area is exhausted of new significant results. Indeed, experiments in progress in our laboratories are producing additional and exciting products, and our belief is that we have seen only the tip of the iceberg in metal/(py)₂CO/carboxylate chemistry in mixed H₂O-organic solvent media using high metal and ancillary ligand to (py)₂CO reaction ratios. As far as future perspectives are concerned, analogues of **1** with other RCO₂⁻ groups are not known to date, and it is currently not evident whether the preparation and stability of such Ni₁₁ clusters are dependent on the particular nature of the R substituent on the carboxylate. The use of other organic solvents (e.g., alcohols, Me₂CO, MeNO₂ . . .), always in combination with H₂O, is also unexplored in this chemistry, and ongoing studies are unearthing interesting new products. Since the μ₃-OH⁻ groups in **1** propagate both antiferromagnetic and ferromagnetic exchange interactions, we also plan to pursue the substitution of the OH⁻ bridges by end-on N₃⁻ groups in order to introduce more or exclusively ferromagnetic components in the superexchange scheme [23,51].

Acknowledgments: Albert Escuer thanks the DGICT project CTQ2015-63614-P for funding. This research has also been co-financed by the European Union (European Social Fund-ESF) and Greek National Funds through the Operational Program “Educational and Lifelong Learning” of the National Strategic Reference Framework (NSRF)-Research Funding Programs: THALES. Investing in knowledge society through the European Social Fund (to Spyros P. Perlepes and Catherine P. Raptopoulou).

Author Contributions: Constantinos G. Efthymiou and Ioannis Mylonas-Margaritis conducted the synthesis and conventional characterization of the cluster; the former also contributed to the interpretation of the results. Catherine P. Raptopoulou and Vassilis Pscharis collected crystallographic data, solved the structure, performed structure refinement, and interpreted structural results; the latter also studied the supramolecular features of the crystal structure and wrote the relevant part of the paper. Albert Escuer performed the magnetic measurements, interpreted the results, and wrote the relevant part of the paper. Constantina Papatriantafyllopoulou and Spyros P. Perlepes coordinated the research, contributed to the interpretation of the results, and wrote parts of the paper.

Conflicts of Interest: The authors declare no conflict of interest.

References

1. Vinslava, A.; Tasiopoulos, A.J.; Wernsdorfer, W.; Abboud, K.A.; Christou, G. Molecules at the Quantum-Classical Nanoparticle Interface: Giant Mn₇₀ Single-Molecule Magnets of ~4 nm Diameter. *Inorg. Chem.* **2016**, *55*, 3419–3430. [[CrossRef](#)] [[PubMed](#)]
2. Brechin, E.K. Using tripodal alcohols to build high-spin molecules and single-molecule magnets. *Chem. Commun.* **2005**, *5141–5153*. [[CrossRef](#)] [[PubMed](#)]
3. Zhang, C.; Chen, C.; Dong, H.; Shen, J.-R.; Dau, H.; Zhao, J. A synthetic Mn₄Ca-cluster mimicking the oxygen-evolving center of photosynthesis. *Science* **2015**, *348*, 690–693. [[CrossRef](#)] [[PubMed](#)]
4. Glatzel, P.; Schroeder, H.; Pushkar, Y.; Boron, T., III; Mukherjee, S.; Christou, G.; Pecoraro, V.L.; Messinger, J.; Yachandra, V.K.; Bergmann, U.; et al. Electronic Structural Changes of Mn in the Oxygen-Evolving Complex of Photosystem II during the Catalytic Cycle. *Inorg. Chem.* **2013**, *52*, 5642–5644. [[CrossRef](#)] [[PubMed](#)]
5. Ako, A.M.; Hewitt, I.J.; Mereacre, V.; Clérac, R.; Wernsdorfer, W.; Anson, C.E.; Powell, A.K. A Ferromagnetically Coupled Mn₁₉ Aggregate with a Record $S = 83/2$ Ground Spin State. *Angew. Chem. Int. Ed.* **2006**, *45*, 4926–4929. [[CrossRef](#)] [[PubMed](#)]
6. Bagai, R.; Christou, G. The *Drosophila* of single-molecule magnetism: [Mn₁₂O₁₂(O₂CR)₁₆(H₂O)₄]. *Chem. Soc. Rev.* **2009**, *38*, 1011–1026. [[CrossRef](#)] [[PubMed](#)]
7. Milios, C.J.; Winpenny, R.E.P. Cluster-Based Single-Molecule Magnets. *Struct. Bond.* **2015**, *164*, 1–109.
8. Evangelisti, M.; Luis, F.; De Jongh, L.J.; Affronte, M. Magnetothermal properties of molecule-based materials. *J. Mater. Chem.* **2006**, *16*, 2534–2549. [[CrossRef](#)]
9. Shaw, R.; Laye, R.H.; Jones, L.F.; Low, D.M.; Talbot-Eeckelaers, C.; Wei, Q.; Milios, C.J.; Teat, S.; Helliwell, M.; Raftery, J.; et al. 1,2,3-Triazolate-Bridged Tetradecametallic Transition Metal Clusters [Mn₁₄(L)₆O₆(OMe)₁₈X₆] (M = Fe^{III}, Cr^{III} and V^{III/IV}) and Related Compounds: Ground-State Spins Ranging from $S = 0$ to $S = 25$ and Spin-Enhanced Magnetocaloric Effect. *Inorg. Chem.* **2007**, *46*, 4968–4978. [[CrossRef](#)] [[PubMed](#)]

10. Carretta, S.; Santini, P.; Amoretti, G.; Affronte, M.; Candini, A.; Ghirri, A.; Tidmarsh, I.S.; Laye, R.H.; Shaw, R.; McInnes, E.J.L. High-Temperature Slow Relaxation of the Magnetization in Ni₁₀ Magnetic Molecules. *Phys. Rev. Lett.* **2006**, *97*, 207201-1–207201-4. [[CrossRef](#)] [[PubMed](#)]
11. Stamatatos, T.C.; Escuer, A.; Abboud, K.A.; Raptopoulou, C.P.; Perlepes, S.P.; Christou, G. Unusual Structural Types in Nickel Cluster Chemistry from the Use of Pyridyl Oximes: Ni₅, Ni₁₂Na₂ and Ni₁₄ Clusters. *Inorg. Chem.* **2008**, *47*, 11825–11838. [[CrossRef](#)] [[PubMed](#)]
12. Papatriantafyllopoulou, C.; Stamatatos, T.C.; Wernsdorfer, W.; Teat, S.J.; Tasiopoulos, A.J.; Escuer, A.; Perlepes, S.P. Combining Azide, Carboxylate, and 2-Pyridyloximate Ligands in Transition-Metal Chemistry: Ferromagnetic Ni^{II}₅ Clusters with a Bowtie Skeleton. *Inorg. Chem.* **2010**, *49*, 10486–10496. [[CrossRef](#)] [[PubMed](#)]
13. Alexopoulou, K.I.; Raptopoulou, C.P.; Psycharis, V.; Terzis, A.; Tangoulis, V.; Stamatatos, T.C.; Perlepes, S.P. Solvent-Dependent Access to Two Different Ni^{II}₄ Core Topologies from the First Use of Pyridine-2,6-dimethanol in Nickel(II) Cluster Chemistry. *Aust. J. Chem.* **2012**, *65*, 1608–1619. [[CrossRef](#)]
14. Perlepe, P.S.; Athanasopoulou, A.A.; Alexopoulou, K.I.; Raptopoulou, C.P.; Psycharis, V.; Escuer, A.; Perlepes, S.P.; Stamatatos, T.C. Structural and magnetic variations in tetranuclear Ni^{II} clusters: the effect of the reaction solvent and ligand substitution on product identity. *Dalton Trans.* **2014**, *43*, 16605–16609. [[CrossRef](#)] [[PubMed](#)]
15. Alexopoulou, K.I.; Terzis, A.; Raptopoulou, C.P.; Psycharis, V.; Escuer, S.P.; Perlepes, S.P. Ni^{II}₂₀ “Bowls” from the Use of Tridentate Schiff Bases. *Inorg. Chem.* **2015**, *54*, 5615–5617. [[CrossRef](#)] [[PubMed](#)]
16. Papaefstathiou, G.S.; Perlepes, S.P. Families of Polynuclear Manganese, Cobalt, Nickel and Copper Complexes Stabilized by Various Forms of Di-2-pyridyl Ketone. *Comments. Inorg. Chem.* **2002**, *23*, 249–274. [[CrossRef](#)]
17. Stamatatos, T.C.; Efthymiou, C.G.; Stoumpos, C.C.; Perlepes, S.P. Adventures in the Coordination Chemistry of Di-2-pyridyl Ketone and Related Ligands: From High-Spin Molecules and Single-Molecule Magnets to Coordination Polymers, and from Structural Aesthetics to an Exciting New Reactivity Chemistry of Coordinated Ligands. *Eur. J. Inorg. Chem.* **2009**, *2009*, 3361–3391.
18. Katsenis, A.D.; Kessler, V.G.; Papaefstathiou, G.S. High-spin Ni(II) clusters: Triangles and planar tetranuclear complexes. *Dalton Trans.* **2011**, *40*, 4590–4598. [[CrossRef](#)] [[PubMed](#)]
19. Jedner, S.B.; Schwöppe, H.; Nimir, H.; Rompel, A.; Brown, D.A.; Krebs, B. Ni(II) complexes as models for inhibited urease. *Inorg. Chim. Acta* **2002**, *340*, 181–186. [[CrossRef](#)]
20. Efthymiou, C.G.; Raptopoulou, C.P.; Terzis, A.; Boča, R.; Korabic, M.; Mrozinski, J.; Perlepes, S.P.; Bakalbassis, E.G. A Systematic Exploration of Nickel(II)/Acetate/Di-2-pyridyl Ketone Chemistry: Neutral and Cationic Clusters, and a Novel Mononuclear Complex. *Eur. J. Inorg. Chem.* **2006**, 2236–2252. [[CrossRef](#)]
21. Tong, M.-L.; Zheng, S.-L.; Shi, J.-X.; Tong, Y.-X.; Lee, H.K.; Chen, X.-M. Synthesis, crystal structures and properties of six cubane-like transition metal complexes of di-2-pyridyl ketone in gem-diol form. *J. Chem. Soc. Dalton Trans.* **2002**, 1727–1734. [[CrossRef](#)]
22. Li, Y.-M.; Zhang, J.-J.; Fu, R.-B.; Xiang, S.-C.; Sheng, T.-L.; Yuan, D.-Q.; Huang, X.-H.; Wu, X.-T. Three new cubane like transition metal complexes of di-2-pyridyl ketone in gem-diol form: Syntheses, crystal structures and properties. *Polyhedron* **2006**, *25*, 1618–1624. [[CrossRef](#)]
23. Papaefstathiou, G.S.; Escuer, E.; Vicente, R.; Font-Bardia, M.; Solans, X.; Perlepes, S.P. Reactivity in polynuclear transition metal chemistry as a means to obtain high-spin molecules: Substitution of μ₄-OH[−] by η¹, μ₄-N₃[−] increases nine times the ground-state S value of a nonanuclear nickel(II) cage. *Chem. Commun.* **2001**, 2414–2415. [[CrossRef](#)]
24. Ji, B.; Deng, D.; Wang, Z.; Liu, X.; Miao, S. Structure of an infinite helical water chain and discrete lattice water in metal-organic framework structures. *Struct. Chem.* **2008**, *19*, 619–623. [[CrossRef](#)]
25. *CrystalClear*; version 1.40; Rigaku/MSC: The Woodlands, TX, USA, 2005.
26. Sheldrick, G.M. *SHELXS 97, Program for Structure Solution*; University of Göttingen: Göttingen, Germany, 1997.
27. Sheldrick, G.M. Crystal structure refinement with SHELXL. *Acta Crystallogr. Sect. C* **2015**, *71*, 3–8. [[CrossRef](#)] [[PubMed](#)]

28. Stamatatos, T.C.; Raptopoulou, C.P.; Perlepes, S.P.; Boudalis, A.K. The first non-acetato members of the bis(anion)octacarboxylatotetrakis{di-2-pyridyl-methanediolate(-2)enneametal(II)} family of complexes: Synthesis, X-ray structures and magnetism of $[M_9(N_3)_2(O_2CCMe_3)_8(py)_2CO_2]_4$ ($M = Co, Ni$). *Polyhedron* **2011**, *30*, 3026–3033. [[CrossRef](#)]
29. Athanasopoulou, A.A.; Pilkington, M.; Raptopoulou, C.P.; Escuer, A.; Stamatatos, T.C. Structural aesthetics in molecular nanoscience: A unique Ni_{26} cluster with a ‘rabbit-face’ topology and a discrete Ni_{18} ‘molecular chain’. *Chem. Commun.* **2014**, *50*, 14942–14945. [[CrossRef](#)] [[PubMed](#)]
30. Foguet-Albiol, D.; Abboud, K.A.; Christou, G. High-nuclearity homometallic iron and nickel clusters: Fe_{22} and Ni_{24} complexes from the use of *N*-methyldiethanolamine. *Chem. Commun.* **2005**, *4282–4284*. [[CrossRef](#)] [[PubMed](#)]
31. Muche, S.; Levacheva, I.; Samsonova, O.; Plam, L.; Christou, G.; Bakowsky, U.; Holyńska, M. A Chiral, Low-Cytotoxic $[Ni_{15}]$ -Wheel Complex. *Inorg. Chem.* **2014**, *53*, 7642–7649. [[CrossRef](#)] [[PubMed](#)]
32. Wix, P.; Kostakis, G.E.; Blatov, V.A.; Proserpio, D.M.; Perlepes, S.P.; Powell, A.K. A Database of Topological Representations of Polynuclear Nickel Compounds. *Eur. J. Inorg. Chem.* **2013**, *2013*, 520–526. [[CrossRef](#)]
33. Dearden, A.L.; Parsons, S.; Winpenny, R.E.P. Synthesis, Structure and Preliminary Magnetic Studies of a Ni_{24} Wheel. *Angw. Chem. Int. Ed.* **2001**, *40*, 152–154. [[CrossRef](#)]
34. Athanasopoulou, A.A.; Raptopoulou, C.P.; Escuer, A.; Stamatatos, T.C. Rare nuclearities in $Ni(II)$ cluster chemistry: A Ni_{11} cage from the first use of *N*-salicylidene-2-amino-5-chlorobenzoic acid in metal cluster chemistry. *RSC Adv.* **2014**, *4*, 12680–12684. [[CrossRef](#)]
35. Brechin, E.K.; Clegg, W.; Murrie, M.; Parsons, S.; Teat, S.J.; Winpenny, R.E.P. Nanoscale Cages of Manganese and Nickel with “Rock Salt” Cores. *J. Am. Chem. Soc.* **1998**, *120*, 7365–7366. [[CrossRef](#)]
36. Brechin, E.K.; Parsons, S.; Winpenny, R.E.P. Uncapped and polar capped prisms of cobalt and nickel. *J. Chem. Soc. Dalton Trans.* **1996**, *3745–3746*. [[CrossRef](#)]
37. Benelli, C.; Blake, A.J.; Brechin, E.K.; Coles, S.J.; Graham, A.; Harris, S.G.; Meier, S.; Parkin, A.; Parsons, S.; Seddon, A.M.; et al. A Family of Polynuclear Cobalt and Nickel Complexes Stabilized by 2-Pyridonate and Carboxylate Ligands. *Chem. Eur. J.* **2000**, *6*, 883–896.
38. Nikiforova, M.E.; Kiskin, M.A.; Bogomyakov, A.S.; Aleksandrov, G.G.; Sidorov, A.A.; Mironov, V.S.; Eremenko, I.L. Synthesis, structure, and magnetic properties of new pyridonate-pivalate nickel(II) complex, $[Ni_{11}(OH)_2(mhp)_8(Piv)_{10}(HCO_2)_2(H_2O)_2(Hmhp)_2(HPiv)_2]$ ($mhp = 6$ -methyl-2-pyridonate), containing formate bridges. *Inorg. Chem. Commun.* **2011**, *14*, 362–365. [[CrossRef](#)]
39. Halcrow, M.A.; Sun, J.-S.; Huffman, J.C.; Christou, G. Structural and Magnetic Properties of $[Ni_4(\mu_3-OMe)_4(dbm)_4(MeOH)_4]$ and $[Ni_4(\eta^1, \mu_3-N_3)_4(dbm)_4(EtOH)_4]$. Magnetostructural Correlations for $[Ni_4X_4]^{4+}$ Cubane Complexes. *Inorg. Chem.* **1995**, *34*, 4167–4177. [[CrossRef](#)]
40. El Fallah, M.S.; Rentschler, E.; Caneschi, A.; Gatteschi, D. Synthesis, crystal structure and magnetic properties of the tetranuclear complex $[Ni_4(OCH_3)_4(dbm)_4(CH_3OH)_4](C_2H_5)_2O$. *Inorg. Chim. Acta* **1996**, *247*, 231–235. [[CrossRef](#)]
41. Escuer, A.; Font-Bardia, M.; Kumar, S.B.; Solans, X.; Vicente, R. Two new nickel(II) cubane compounds derived from pyridine-2-methoxide (Pym): $\{Ni_4(Pym)_4Cl_4(CH_3OH)_4\}$ and $\{Ni_4(Pym)_4(N_3)_4(CH_3OH)_4\}$. Crystal structures and magnetic properties. *Polyhedron* **1999**, *18*, 909–914. [[CrossRef](#)]
42. Clemente-Juan, J.M.; Chansou, B.; Donnadieu, B.; Tuchagues, J.-P. Synthesis, Structure, and Magnetic Properties of the Low-Symmetry Tetranuclear Cubane-like Nickel Complex $[Ni_4(pypentO)(pym)(\mu_3-OH)_2(\mu_3-Oac)_2(NCS)_2(OH)_2]$. *Inorg. Chem.* **2000**, *39*, 5515–5519. [[CrossRef](#)] [[PubMed](#)]
43. Boskovic, C.; Rusanov, E.; Stoeckli-Evans, H.; Güdel, H.U. New tri- and tetranuclear transition metal spin clusters incorporating a versatile polydentate Schiff base ligand. *Inorg. Chem. Commun.* **2002**, *5*, 881–886. [[CrossRef](#)]
44. Mukherjee, S.; Weyhermüller, T.; Bothe, E.; Wieghardt, K.; Chaudhuri, P. Single-Atom O-Bridged Urea in a Dinickel(II) Complex with Ni^{II}_4 , Cu^{II}_2 and Cu^{II}_4 Complexes of a Pentadentate Phenol-Containing Schiff Base with (O,N,O,N,O)-Donor Atoms. *Eur. J. Inorg. Chem.* **2003**, *863–875*. [[CrossRef](#)]
45. Paine, T.K.; Rentschler, E.; Weyhermüller, T.; Chaudhuri, P. Polynuclear Nickel(II) Complexes: Preparation and Magnetic Properties of Ni^{II}_4 , Ni^{II}_5 and Ni^{II}_6 Species with Ligands containing OXO ($X = S, Se$, or N) Donor Atoms. *Eur. J. Inorg. Chem.* **2003**, *3167–3178*. [[CrossRef](#)]

46. Aromi, G.; Batsanov, A.S.; Christian, P.; Helliwell, M.; Roubeau, O.; Timco, G.A.; Winpenny, R.E.P. Synthesis, structure and magnetic properties of hydroxyquininaldine-bridged cobalt and nickel cubanes. *Dalton Trans.* **2003**, *4466–4471*. [[CrossRef](#)]
47. Moragues-Cánovas, M.; Helliwell, M.; Ricard, L.; Rivière, E.; Wernsdorfer, W.; Brechin, E.; Mallah, T. An Ni_4 Single-Molecule Magnet: Synthesis, Structure and Low-Temperature Magnetic Behaviour. *Eur. J. Inorg. Chem.* **2004**, *2014*, *2219–2222*. [[CrossRef](#)]
48. Papaefstathiou, G.S.; Escuer, A.; Mautner, F.A.; Raptopoulou, G.; Terzis, A.; Perlepes, S.P.; Vicente, R. Use of the Di-2-pyridyl Ketone/Acetate/ Dicyanamide “Blend” in Manganese(II), Cobalt(II) and Nickel(II) Chemistry: Neutral Cubane Complexes. *Eur. J. Inorg. Chem.* **2005**, *879–893*. [[CrossRef](#)]
49. Papatriantafyllopoulou, C.; Efthymiou, C.G.; Raptopoulou, C.P.; Vicente, R.; Manessi-Zoupa, E.; Pscharis, V.; Escuer, A.; Perlepes, S.P. Initial use of the di-2-pyridyl ketone/sulfate “blend” in 3d-metal cluster chemistry: Preparation, X-ray structures and physical studies of zinc(II) and nickel(II) cubanes. *J. Mol. Struct.* **2007**, *829*, *176–188*. [[CrossRef](#)]
50. Chilton, N.F.; Anderson, R.P.; Turner, L.D.; Soncini, A.; Murrax, K.S. PHI: A Powerful New Program for the Analysis of Anisotropic Monomeric and Exchange-Coupled Polynuclear d- and f-block Complexes. *J. Comput. Chem.* **2013**, *34*, *1164–1175*. [[CrossRef](#)] [[PubMed](#)]
51. Papaefstathiou, G.S.; Perlepes, S.P.; Escuer, A.; Vicente, R.; Font-Bardia, M.; Solans, X. Unique Single-Atom Binding of Pseudohalogeno Ligands to Four Metal Ions Induced by Their Trapping into High-Nuclearity Cages. *Angew. Chem. Int. Ed.* **2001**, *40*, *884–886*. [[CrossRef](#)]



© 2016 by the authors; licensee MDPI, Basel, Switzerland. This article is an open access article distributed under the terms and conditions of the Creative Commons Attribution (CC-BY) license (<http://creativecommons.org/licenses/by/4.0/>).